Large 3D bioprinted tissue: Heterogeneous perfusion and vascularization

Léa Pourchet, Emma Petiot, Céline Loubière, Éric Olmos, Morgan dos Santos, Amélie Thepot, Blum Loïc, Frédérique Depierre, Christophe Marquette

LARGE 3D BIOPRINTED TISSUE: DYNAMIC MATURATION AND VASCULARIZATION

Lea Pourchet[1], Emma Petiot[1], Céline Loubière[3], Eric Olmos[3], Morgan Dos Santos[2], Amélie Thépot[2], Blum J. Loïc[1] and Christophe A. Marquette[1*]

[1.] 3d.FAB, Univ Lyon, Université Lyon1, CNRS, INSA, CPE-Lyon, ICBMS, UMR 5246, Bat. Lederer, 1 rue Victor Grignard, 69100 Villeurbanne, France.
christophe.marquette@univ-lyon1.fr

[2.] LabSkin Creations, Edouard Herriot Hospital, 5 place d'Arsonval, Bâtiment 5, 69437, Lyon, France.

[3] Laboratoire Réactions et Génie des Procédés, Université de Lorraine, CNRS, LRGP, F-54000 Nancy, France

Abstract

Large bioprinted tissues (dm^3) are being more and more accessible but their *in vitro* culture and maturation conditions are still an unknown territory. In the present report, we are presenting a preliminary study of endothelialized large bioprinted tissues (fibroblast and human dermal microvascular endothelial cells) maturation using silicone 3D printed bioreactors. Computational Fluid Dynamics (CFD) simulation was used to link the theoretical culture medium flow path within the large bioprinted tissue with the actual tissue morphology and composition, obtained through histological observations. The obtained results demonstrate the positive impact of using dynamic maturation conditions (300 mL/h culture medium flow rate) on the extracellular matrix production and the conservation of the large bioprinted tissue internal geometry. Clear differences between static and dynamic culture conditions were herein found. Finally, typical microvascular organization, composed of human dermal microvascular endothelial cells organized around an open lumen, were found within the large bioprinted tissue.

Keywords: 3D bioprinting; bioreactor; Computational Fluid Dynamics; endothelial cells; fibroblasts; microvascularization.

1. Introduction

Bioprinting became in the last 5 years a highly active scientific area in which multidisciplinary expertise was the key to the success[1]. Nevertheless, the expectations of the field for regenerative medicine applications involving large living tissues (in the cm^3 to dm^3 range) were far than fulfill, mainly because of the vascularization issues related to large tissue or organ *in vitro* maturation. A strong effort might then be placed in scaling-up processes applicable to customized tissues production[2]. Just like for bioengineering 40 years ago, this scale-up will have to go through specific and controlled bioreactors developments. For a better understanding, defining the word bioreactor is essential. Martin et al.[3] defined it as devices in which biological and/or biochemical processes operate under closely monitored and tightly controlled environmental and operating conditions (e.g., pH, temperature, pressure, nutrient supply, and waste removal). Conventionally, bioreactor studies may be separated into two groups: bioreactor for cell culture (either suspension or 2D adherent cells) and bioreactor for *in vitro* tissues maturation. While the first group already benefits from abundant literature, for example for virus or active biomolecule productions[4], the second one lacks adaptability, particularly when it comes to specific tissue maturation conditions (mechanical stress, perfusion) but also to the actual design and shape of the targeted tissue or organ. One of the seldom example is the work by Olivier et al.[5] who created a specific maturation bioreactor for large bone defects.

In one of our previous work, the achievement of 3D bioprinted skin patches (cm^2), recapitulating dermis/epidermis structure and composition, was demonstrated[6]. Nevertheless, the size and thickness of these bioprinted tissues were limited by i) the available classical *in vitro* cell culture tools and ii) the corresponding static culture conditions, which both hindered the development of dm^3 vascularized tissues. Indeed, this micro- and macro- vascularization will have a direct impact on our capacity to scale-up tissue engineering while maintaining cell viability through continuous nutriment supply flow.

The primary goal of the present work was to evaluate possible efficient avenues for the production of dm^3 bioprinted tissues through: i) internal tissue geometry leading to easy culture medium perfusion and ii) on demand bioreactors design perfectly fitting the size and shape of bioprinted tissues. These bioreactors are used both to allow the maturation of large bioprinted tissues in dynamic conditions and to induce vascularization. Our secondary goal was to obtain macroscopic organization of the tissue thanks to the internal lattice of the 3D bioprinting together with a correct arrangement at the cellular level. In other words, a microvascularisation (cells self-organization) connected to macrovascularisation (3D printed internal structures). A complementary approach based on Computational Fluid Dynamics (CFD) simulation was used to link the theoretical culture medium flow path within the large bioprinted tissue with the actual tissue morphology and composition.

2. Materials and Methods

2.1. Cells' isolation and cultivation

Foreskin samples were obtained from healthy patients undergoing circumcision, according to French regulation including declaration to ministry (DC No. 2014- 2281) and procurement of written informed consent from the patient. Fibroblasts were isolated from 2 years-old donor and cultivated in flasks at 37°C, 5% CO_2 in Dulbecco's modified Eagle medium (DMEM)/Glutamax TM-1 medium (Gibco Cell Culture, Invitrogen, France), supplemented with 10% calf bovine serum (HyClone™, GE Healthcare Life Sciences, France), 1% penicillin, streptomycin and amphotericin B (Bio Industries-Cliniscience, France). Culture medium was changed every 2 days and cells were routinely passaged in culture flasks until bioprinting. Cells of passages between 7 and 9 were used.
Human dermal microvascular endothelial cells expressing GFP were kindly supplied by Dr. Jean-Jacques Feige[7] and cultivated in the same conditions as fibroblasts.

2.2. Bioink formulation

Bioink consisted in a mixture of 10% (w/v) bovine gelatine (Sigma-Aldrich, France), 2% (w/v) fibrinogen (Sigma-Aldrich, France) and 0.5% (w/v) very low viscosity alginate (Alpha Aesar, France) dissolved in NaCl 0.9% (Laboratoire Aguettant, France), as already described[6]. Bioprinted large tissues were then immerged during 1 h at room temperature in a 0.05% (w/v) thrombin (30-400 NIH/mg, Sigma Aldrich, France) / 3% (w/v) calcium chloride (Sigma Aldrich, France) solution to polymerize fibrinogen and alginate.

2.3. Histological and immunohistochemical analysis

After 7 days of maturation, large bioprinted tissues were immediately fixed in 4% formalin and embedded in paraffin. Paraffin-embedded formalin-fixed samples were then cut into 3 µm sections. After dewaxing and rehydration, sections were stained with Masson's Trichrome (light green) for routine histology. For immunohistochemistry, labelling was performed on 5 µm sections and incubated with anti-endothelium EN4 mouse monoclonal primary antibody (ABCAM ab8087). A staining kit (ImmPRES™ excel staining kit-7602) was used as a secondary antibody and incubated for 1 hour at room temperature. A nuclear counterstaining was performed using Harris Hematoxylin.
Specimens stained in Masson's Trichrome were observed using an optical microscope, and images were captured using DSU-3 camera and NIS-Elements software.

Immunohistochemistry specimens were visualized using a Nikon Eclipse Ts2R inverted microscope and images were captured using DS-Fi3 high-definition colour camera. Eight-bit images were saved in an uncompressed image file format (lsm).

2.4. Computational Fluid Dynamics (CFD)

CFD simulations were performed by using the commercial finite solver ANSYS Fluent and data post-treatment was realized by using the software CFD-Post (ANSYS Inc., version 16.1). The steady-state approach was sued and the flow was supposed laminar. A wall boundary condition, i.e. zero-velocity, was applied for bioreactor boundaries and tissue zones. The mass and momentum conservation equations (Eq. (1) and (2)) were solved for the liquid phase supposing water properties at 37°C (density ρ = 993 kg m^{-3} and dynamic viscosity $\mu = 6.92 \times 10^{-4}$ Pa s^{-1}), with $\boldsymbol{v}$ is the fluid velocity, p the pressure and $\boldsymbol{g}$ the acceleration due to gravity.

$$\nabla \cdot (\rho \boldsymbol{v}) = 0 \quad (1)$$

$$\nabla \cdot (\rho \boldsymbol{v}\boldsymbol{v}) = -\nabla p - \nabla \cdot \bar{\bar{\boldsymbol{\tau}}} + \rho \boldsymbol{g} \quad (2)$$

The calculation mesh consisted in 19 millions of tetrahedral meshes approximately. Pressure-velocity coupling was solved using a SIMPLE method and pressure and momentum transport equations were discretized using 2nd order UPWIND schemes. Convergence of the simulations was verified by monitoring liquid velocities till complete stabilization.

3. Results

Taking full advantage of the latest developments in 3D printing, the proposed approach consists in producing both the bioreactor vessel (container) and the living tissue using additive manufacturing techniques. The bioreactors are then printed through silicone (Sikasil®-C, SIKA, Swiss) cold extrusion printing, while the tissues are printed using cold extrusion bioprinting. This approach, consisting in 3D printing both the reagent cartridge and the living tissue, has been introduced by Jennifer Lewis group in 2016 in a study where fugitive ink was used to produce hollow networks connected to a perfusion system[8]. This pioneer work was an attempt in building a vascular network of controlled shape and structure within a cm^3 living tissue. The present work is a complementary study where the bioprinted tissue is specifically shaped to enable perfusion.

The silicone bioreactor was printed in a way that enables to freely choose the inlet and outlet position of the flow through needle puncture in the silicone (**Figure 1-A**). An additional acrylate cover, connected to a sterile filter for vent and gas exchange was printed using a commercially available inkjet printer (Objet Pro, Stratasys, France; VeroClear RGD810). Acrylate cover was extensively washed in 70% v/v ethanol/water for five days to remove any traces of toxic residues (acrylate monomers and photoinitiators) prior cell culture. The CAD file of the complete set-up can be found in an open source format at https://gist.github.com/FabricAdvancedBiology.

The large bioprinted tissue was here 8 cm^3 (2x2x2 cm) and composed of 1 million fibroblasts (normal human dermal fibroblasts from young donor, 2 y.o. prepared according to Shahabeddin et al.[9]) and 5 million human dermal microvascular endothelial cells (hDMEC). Fibroblasts were herein used for their capacity to produce rapidly a well-organized extracellular matrix (ECM) network, thus consolidating the printed object. The endothelial cells were used to initiate the recapitulation of microvascular structures. Bioprinting of the tissue was performed using our in-house developed bioprinter (TOBECA, France[6]), a tronconical nozzle with inner diameter of 400 µm (Nordson, USA) and our previously published optimized bioink[6]. The large bioprinted tissue was produced with an internal lattice leaving 80% of the object volume open to culture medium diffusion (**Figure 1-B, C)**.

This 20% infill leads to the production of millimeters size macro-porosity within the tissue. Additional solid walls were printed on four perimeters of the object to orientate flow in one direction within the object. Computational Fluid Dynamics (CFD) was used to simulate the culture medium flow within the large bioprinted tissue. As depicted in **Figure 1-D**, flow conditions and object internal shape, leading to heterogeneous fluid flow velocities (and then residence time) within the bioprinted tissue and a large residence time distribution, were chosen as an attempt to create a 3D preferential development within the tissue. As can be seen, a clear preferential path was created with low residency times and high velocities (see ***Supplementary Information 1***).

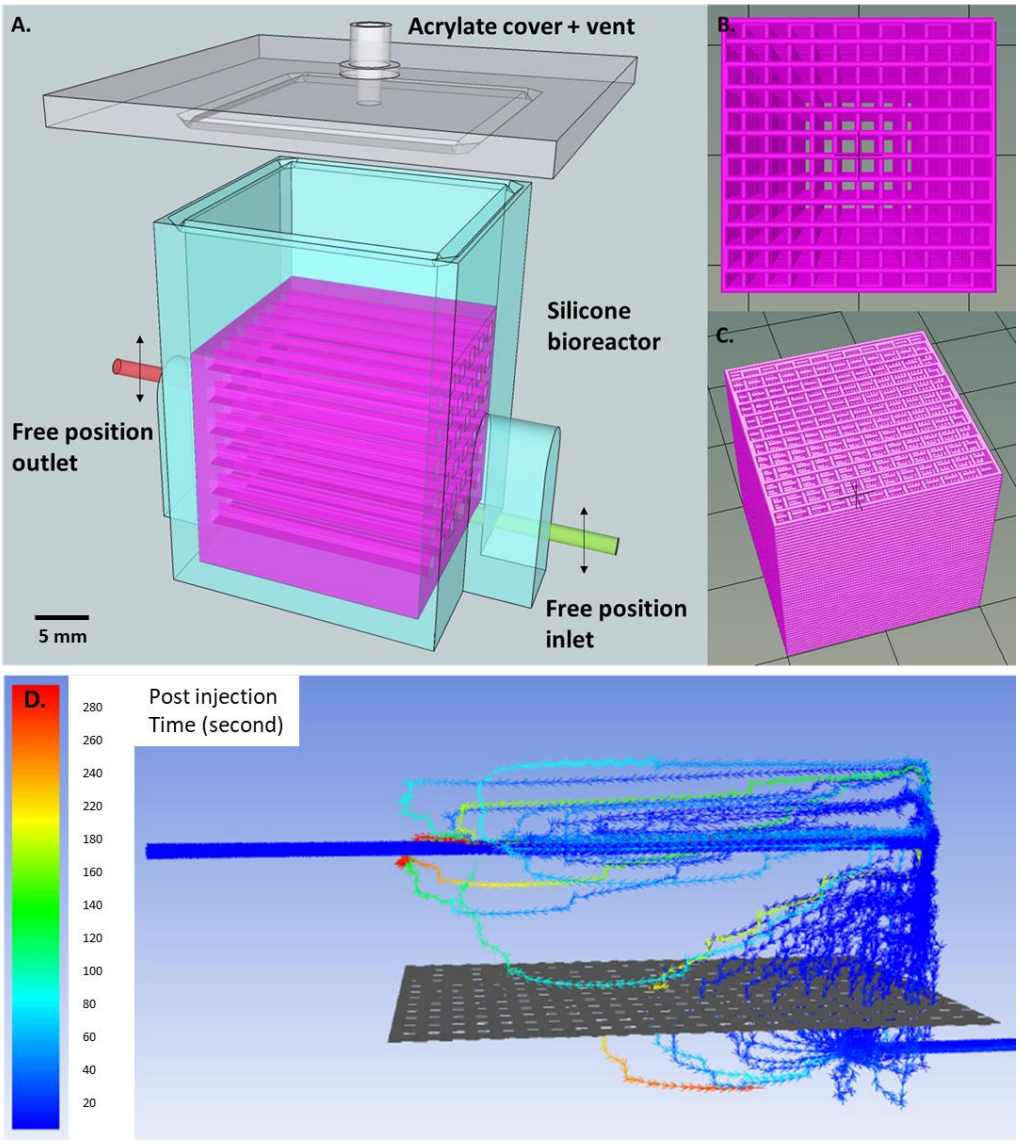

Figure 1. A. view of the 3D printed bioreactor with its inlet and outlet free positioning (through needle puncture). B. and C. 3D view of the bioprinted large tissue showing internal macro-porosity. D. Pathlines of liquid flow within the bioreactor. Colors represent post injection time, i.e. time necessary to a finite element to reach a particular position within the large bioprinted tissue.

The large bioprinted tissue was then cultured 12 days in the bioreactor using an inlet flowrate of 300 mL/h (Peristaltic Pump P-1, GE Healthcare Life Science) of culture medium with daily injection of vitamin C (50 µg/mL final concentration), a well-known fibroblast growth factor used to trigger extra-cellular matrix secretion [10]. In order to permit temperature control and pH buffering within the bioreactor, this latter was placed directly in a standard CO_2 cell culture incubator.

After one week of dynamic culture, the tissue exhibited a clear isomorphic volume reduction (from 8 cm^3 to 6 cm^3), typical of the fibroblast based tissue maturation in which newly synthetized ECM and cells' attachment induces retraction[11]. This ECM production was evidenced in **Figure 2-B** through Masson's Trichrome staining. **Figure 2-B** also depicted the internal macro-porosity of the large bioprinted tissue. As a matter of fact, the initial millimetre size porosity was conserved during the dynamic tissue maturation, leading to tubular structures within the bioprinted tissue orientated toward the perfusion flow direction and perpendicular to the 3 µm histological section. Comparing the heterogeneity of the obtained extracellular matrix production and the flow velocity distribution within the object showed a clear link between both phenomena (**Figure 2-B** and **2-C**). Indeed, zone-A ECM production was found to be very low with a clear impact of the position of the needle entry. Then, zone-B, which is characterized by a wider spreading of the flow velocity, evidenced a more homogeneous ECM production. Finally, in agreement with the flow and post injection time (**Figure 1-D**), zone-C depicted the most intense and homogeneous ECM production.

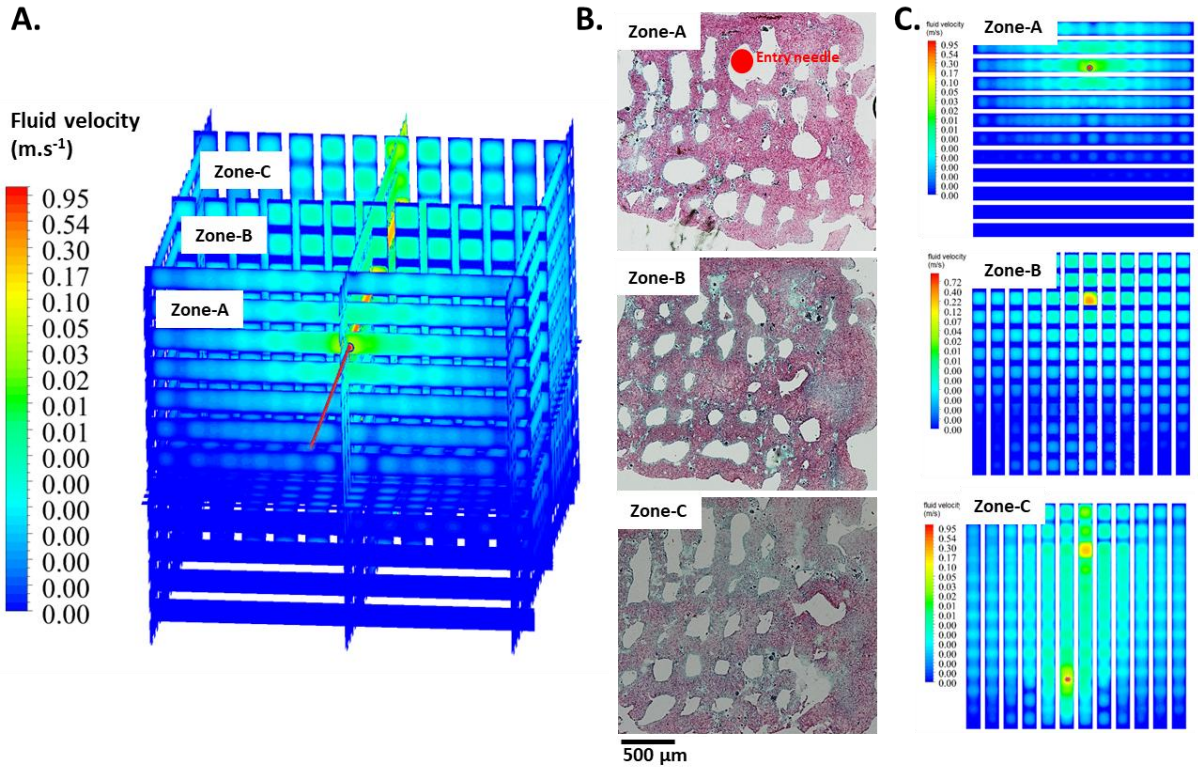

Figure 2 A: Fluid flow velocity fields from CFD simulation of three different zones within the large bioprinted tissue. B: Characterization of 5 µm sections of the bioprinted large tissue after 12 days of dynamic culture. Full-size view of the large bioprinted tissue (Masson's Trichrome). C: Corresponding fluid flow velocity fields from simulation, in each zone.

Taking a closer view at the tissue structuration and composition using **Figure 3-A** histological micrographs, the tissue was shown to be fully colonized by viable and spread cells surrounded by green staining, proof of the presence of neo-synthetized ECM and collagen secreted by the fibroblasts. It is also worth to mention that the large bioprinted tissue evidenced a strong accumulation of cells and ECM at the interface between the printed object and the culture medium. These cells were identified, using hematoxylin counterstaining and EN4 immunohistochemistry labelling, to be preferentially fibroblast at the interface (no EN4 labelling, violet staining of the nuclei), whereas human dermal microvascular endothelial cells were found to be distributed within the tissue (brown EN4 labelling) (**Figure 3-B**).

The presence of the human dermal microvascular endothelial cells was also observed through fluorescent optical microscopy of the whole bioprinted tissue (**Figure 3-C**). As can be seen, numerous fluorescent microstructures were found within the bioprinted large tissue, with clear interconnected tubular organization. Finally, the large bioprinted tissue was search for the presence of typical microvascular organization composed of human dermal microvascular endothelial cells organized around an open lumen [12]. Two examples of such organization are presented in **Figure 3-D**. Typical micro vessel were thus found with lumen inner diameters between 5 and 25 µm.

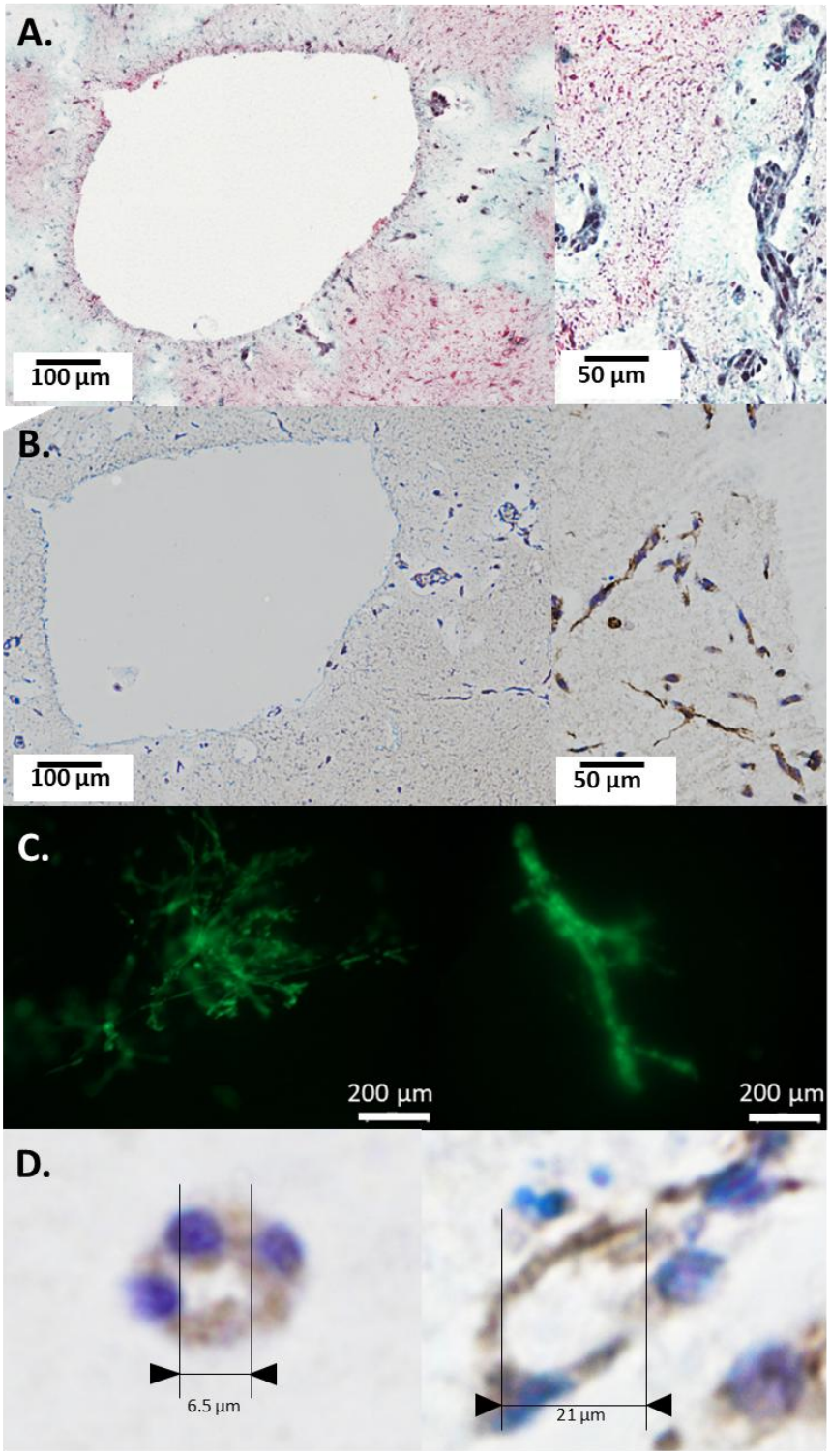

Figure 3 Histological and immunohistological characterizations of 5 µm sections of the bioprinted large tissue after 7 days of dynamic culture. A: Masson's Trichrome staining of perfusion pore and a closer view of the surrounding tissue (violet staining of nuclei, green staining of collagen or ECM). B: EN4 immunohistochemistry staining (brown cytoplasmic staining) of the same perfusion pore and a closer view of the same surrounding tissue. C: Fluorescent microscopy images showing human dermal microvascular endothelial cells network. D: EN4 immunohistochemistry staining of human dermal microvascular endothelial cells organized around an open lumen.

For sake of comparison and in an attempt to identify the impact of the use of dynamic culture conditions on the large bioprinted tissue maturation, a control experiment was performed using an identical large bioprinted tissue matured in static culture conditions, i.e. no perfusion flow. First important observation is the poor shape conservation of the internal initial millimetre size porosity with only seldom remaining tubular structures (**Supplementary Information 2-A**). Then, the typical fibroblast's tissue retraction[13] observed for the tissue cultures under dynamic conditions (retraction factor of 70%), is here much lesser with a retraction factor of only 10%. Also, as can be observed (**Supplementary Information 2-B**), a clearly lower density of extracellular matrix was produced under static culture conditions with only seldom dense, green staining. These two observations are of course related since *in vivo*, different proteins secreted by fibroblasts progressively accumulate and organize to create networks connecting fibroblasts together and to their environment[14, 15], leading to tissue retraction *in vitro*. Lower extracellular matrix density implies then lower tissue retraction during maturation.

When it comes to the observation of the human dermal microvascular endothelial cells within the tissue, clear organization in connected cell networks was evidenced but with, in addition, the presence of endothelial cell spheroids (red arrows pointing spheroids in **Supplementary Information 2-C**). Finally, when searching the presence of lumen based microvascular organization within this large bioprinted tissue matured under static conditions, no such structure can be identified, suggesting an incomplete maturation of the endothelial cells' network.

4. Conclusions

From all these observations, a first conclusion can me made about the impact of the dynamic culture on the possibility to generate and maintain millimeter size tubular structures within a dm^3 bioprinted tissue. Indeed, identical tissues shown significantly different evolutions of their internal geometry when submitted or not to a constant perfusion flow. This result is clearly related to the hydromechanical stress generated by the medium solution flowing within the millimeter size internal structure of the bioprinted object.

At the extracellular matrix level, the lower production level of collagen within the bioprinted tissue cultured under static conditions clearly indicates a lower maturation rate of the tissue (collagen production by human fibroblasts), certainly related to a poor conservation of its internal porosity, leading to a hindered culture medium diffusion within the tissue. Then, analyzing the human dermal microvascular endothelial cells' organization, a clear difference was observed between dynamic and static culture conditions. The later leading to less micro-structured network organization, no lumen based microstructures and the presence of spheroids, typical of environmental stress of the cells[16, 17]. This observation has to be linked to the lower ECM production within the large bioprinted tissue matured under static and the fact that the ECM or at least adhesion peptide content, impacts directly the behavior of the embedded cells which might either adhere and spread, forming organized tissue structure, or regroup and form spheroids.

The results presented in this short study were meant to evaluate the impact of the concomitant use of an oriented internal millimeter size porosity and dynamic culture conditions (perfusion) on the

maturation of a large bioprinted tissue (dm^3) incorporating cell components useful for micro-vascularization development (human dermal microvascular endothelial cells). The obtained results clearly indicate that the developed procedure enables in one hand the conservation of the internal porosity of the bioprinted tissue, leading to a constant and homogeneous perfusion of the entire tissue, and in the other hand the development of a clear organization in connected endothelial cell networks. Of course, numerous studies might now be performed to clarify whether or not the produced endothelial cell network can be matured toward a connection to the perfusion network, but these preliminary results are of great impact in the field since dm^3 vascularized bioprinted tissues maturation is expected to be next breakthrough in tissue engineering.

Acknowledgement

This work was supported by the French ANR program ASTRID (project BLOC-PRINT - ANR-16-ASTR-0021), led and funded by the Direction Générale de l'Armement (DGA). The authors also sincerely thank Dr. Jean-Jacques Feige (CEA/DRF/BIG/BCI) for supplying human dermal microvascular endothelial cells (hDMEC) expressing GFP.

References

1. Seol, Y.J., et al., *Bioprinting technology and its applications.* European Journal of Cardio-Thoracic Surgery, 2014. **46**(3): p. 342-348.
2. Gelinsky, M., A. Bernhardt, and F. Milan, *Bioreactors in tissue engineering: Advances in stem cell culture and three-dimensional tissue constructs.* Engineering in Life Sciences, 2015. **15**(7): p. 670-677.
3. Martin, I., D. Wendt, and M. Heberer, *The role of bioreactors in tissue engineering.* Trends in Biotechnology, 2004. **22**(2): p. 80-86.
4. Gallo-Ramirez, L.E., et al., *Bioreactor concepts for cell culture-based viral vaccine production.* Expert Review of Vaccines, 2015. **14**(9): p. 1181-1195.
5. Olivier, V., et al., *In vitro culture of large bone substitutes in a new bioreactor: importance of the flow direction.* Biomedical Materials, 2007. **2**(3): p. 174-180.
6. Pourchet, L.J., et al., *Human Skin 3D Bioprinting Using Scaffold-Free Approach.* Adv Healthc Mater, 2017. **6**(4).
7. Desroches-Castan, A., et al., *A new chemical inhibitor of angiogenesis and tumorigenesis that targets the VEGF signaling pathway upstream of Ras.* Oncotarget, 2015. **6**(7): p. 5382-5411.
8. Kolesky, D.B., et al., *Three-dimensional bioprinting of thick vascularized tissues.* Proceedings of the National Academy of Sciences of the United States of America, 2016. **113**(12): p. 3179-3184.
9. Shahabeddin, L., et al., *Characterization of skin reconstructed on a chitosan-cross-linked collagen-glycosaminoglycan matrix.* Skin Pharmacol, 1990. **3**(2): p. 107-14.
10. Geesin, J.C., et al., *Ascorbic Acid Specifically Increases Type I and Type III Procollagen Messenger RNA Levels in Human Skin Fibroblasts.* Journal of Investigative Dermatology, 1988. **90**(4): p. 420-424.
11. Gauvin, R., et al., *Minimal contraction for tissue-engineered skin substitutes when matured at the air–liquid interface.* Journal of Tissue Engineering and Regenerative Medicine, 2013. **7**(6): p. 452-460.
12. Ayata, R.E., et al., *Behaviour of Endothelial Cells in a Tridimensional In Vitro Environment.* BioMed Research International, 2015. **2015**: p. 9.
13. Lee, V., et al., *Design and fabrication of human skin by three-dimensional bioprinting.* Tissue engineering. Part C, Methods, 2014. **20**(6): p. 473-484.
14. Kolarsick, P.A.J., M.A. Kolarsick, and C. Goodwin, *Anatomy and Physiology of the Skin.* Journal of the Dermatology Nurses' Association, 2011. **3**(4): p. 203-213.

15. Marcos-Garcés, V., et al., *Age-related dermal collagen changes during development, maturation and ageing – a morphometric and comparative study.* Journal of Anatomy, 2014. **225**(1): p. 98-108.
16. Tseng, T.-C., et al., *Biomaterial Substrate-Mediated Multicellular Spheroid Formation and Their Applications in Tissue Engineering.* Biotechnology Journal, 2017. **12**(12): p. 1700064-n/a.
17. Shu, X.Z., et al., *Attachment and spreading of fibroblasts on an RGD peptide-modified injectable hyaluronan hydrogel.* Journal of Biomedical Materials Research Part A, 2004. **68A**(2): p. 365-375.